Supporting Information

Boosting photocatalytic CO_2 reduction via Schottky junction with ZnCr layered double hydroxide nanoflakes aggregated on 2D $Ti_3C_2T_x$ cocatalyst

Boye Zhou,[a,b] Yong Yang,*[c] Zhengchu Liu,[a,b] Niandu Wu,[a] Yuxiang Yan,[a] Wenhua Zhao,[a] Huichao He,[d] Jun Du,[a] Yongcai Zhang,[e] Yong Zhou*[a,b,f] and Zhigang Zou[a,b,f]

[a] *National Laboratory of Solid State Microstructures, Collaborative Innovation Center of Advanced Microstructures, School of Physics, Nanjing University, Nanjing 210093, P. R. China. E-mail: zhouyong1999@nju.edu.cn*

[b] *Eco-Materials and Renewable Energy Research Center (ERERC), Jiangsu Key Laboratory for Nano Technology, Nanjing University, Nanjing, 210093, China*

[c] *Key Laboratory of Soft Chemistry and Functional Materials (MOE), Nanjing University of Science and Technology, Nanjing 210094, P. R. China. E-mail: yychem@njust.edu.cn*

[d] *Institute of Environmental Energy Materials and Intelligent Devices, School of Metallurgy and Materials Engineering, Chongqing University of Science and Technology. Chongqing 401331, China*

[e] *Yangzhou University, School of Chemical Engineering, Yangzhou 225002, P. R. China*

[f] *School of Science and Engineering, The Chinese University of Hongkong (Shenzhen), Shenzhen, Guangdong 518172, China*

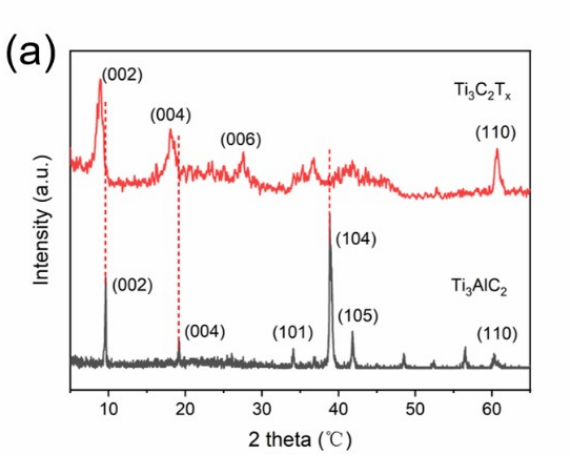

Figure S1. XRD patterns of Ti_3AlC_2 and $Ti_3C_2T_x$.

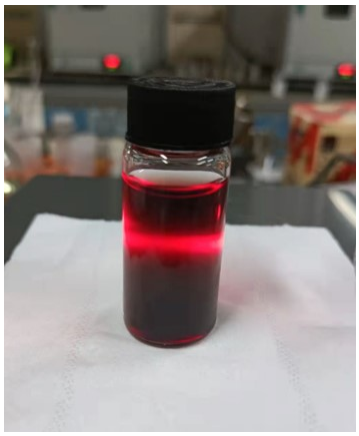

Figure S2. The ‘black’ colloid dispersion of $Ti_3C_2T_x$ nanosheets.

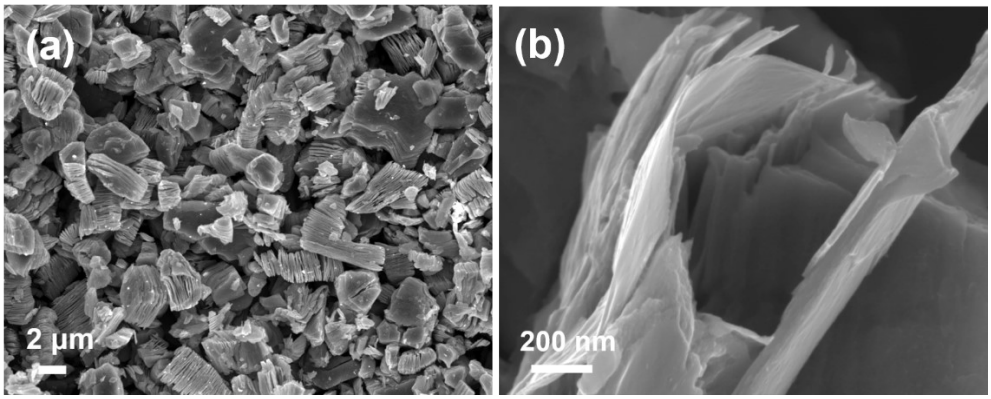

Figure S3. (a) Bulk $Ti_3C_2T_x$; (b) delaminated thinner $Ti_3C_2T_x$ nanosheets.

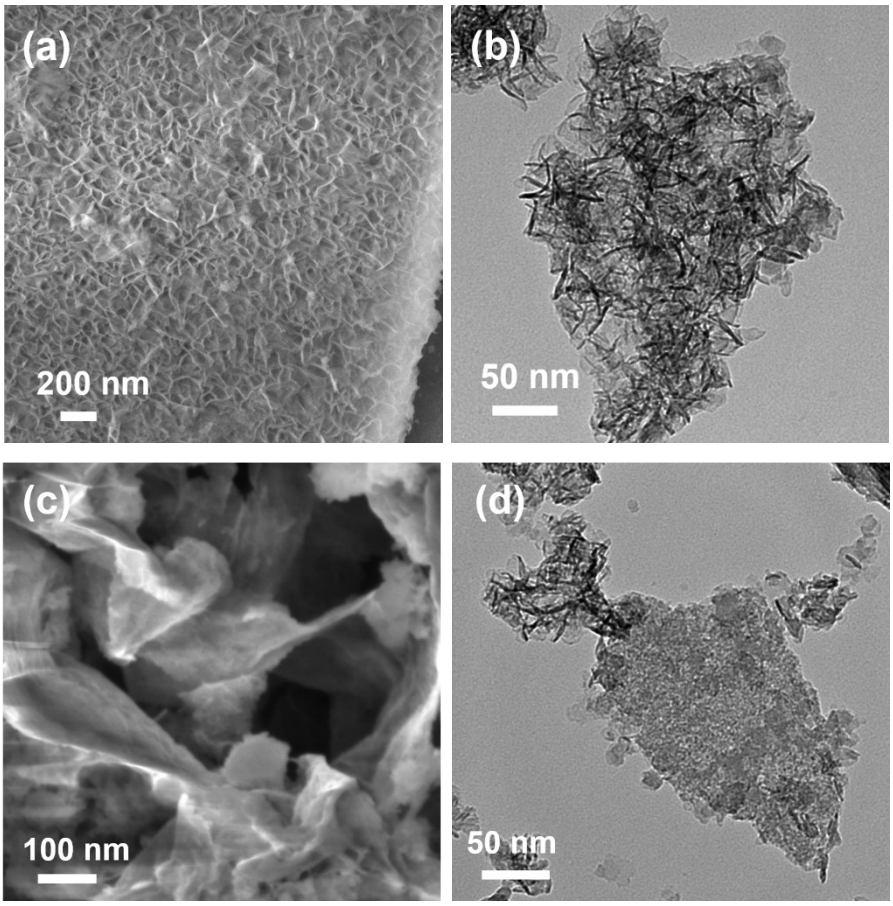

Figure S4. (a, b) SEM and TEM image of self-assembled ZnCr-LDH, respectively. (c,d) SEM and TEM image of ZCTC25, respectively.

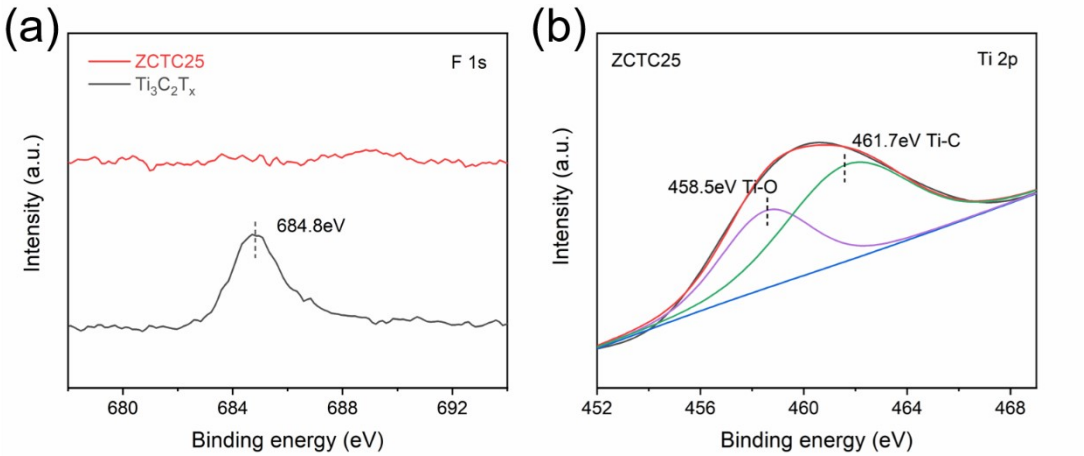

Figure S5. (a) High-resolution XPS F 1s spectrum of ZCTC25 and $Ti_3C_2T_x$. (b) High-resolution XPS Ti 2p spectrum of ZCTC25.

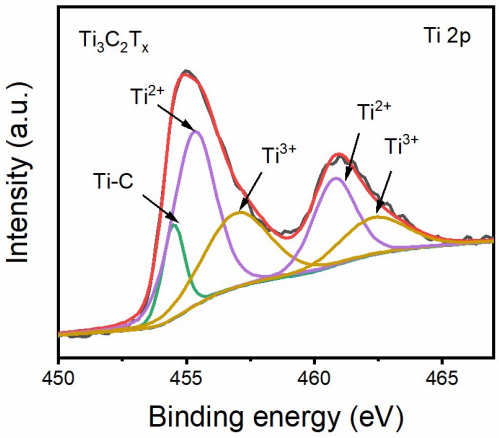

Figure S6. High-resolution XPS Ti 2p spectrum of $Ti_3C_2T_x$.

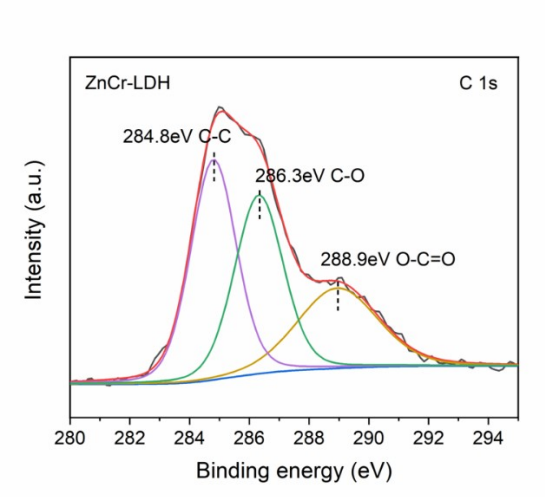

Figure S7. High-resolution XPS C 1s spectrum of ZnCr-LDH.

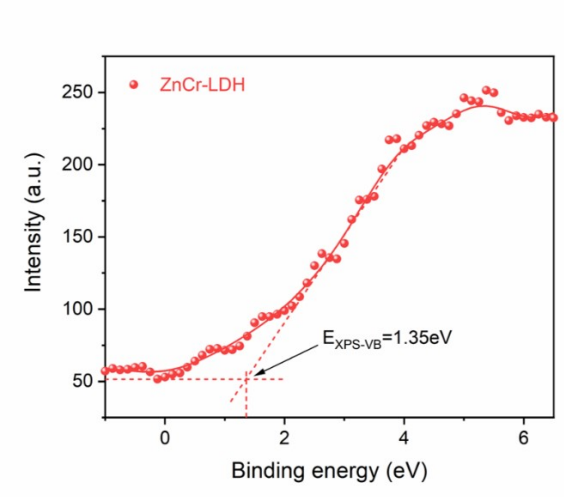

Figure S8. High-resolution XPS valence band spectrum of ZnCr-LDH.

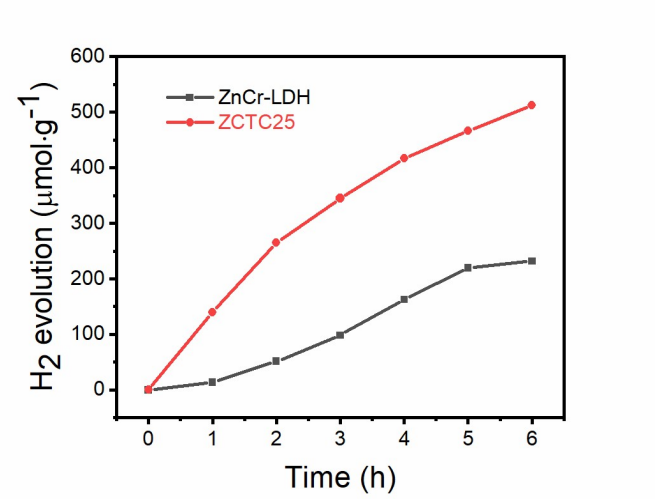

Figure S9. H_2 evolution of ZnCr-LDH and ZCTC25.

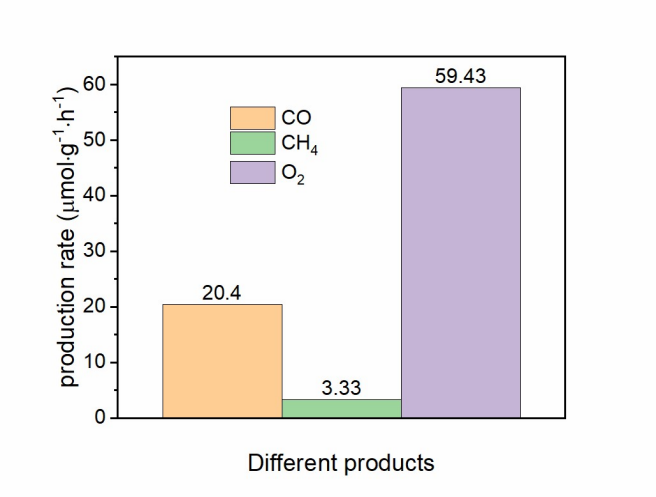

Figure S10. The production rate of different products of ZCTC25.

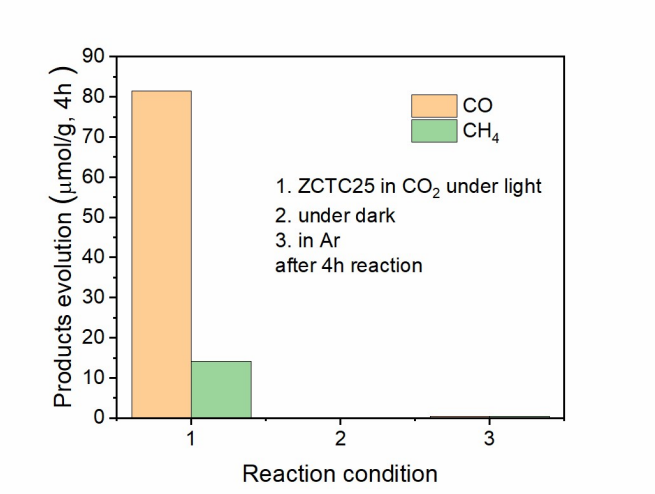

Figure S11. The production of CO and CH_4 under different conditions.

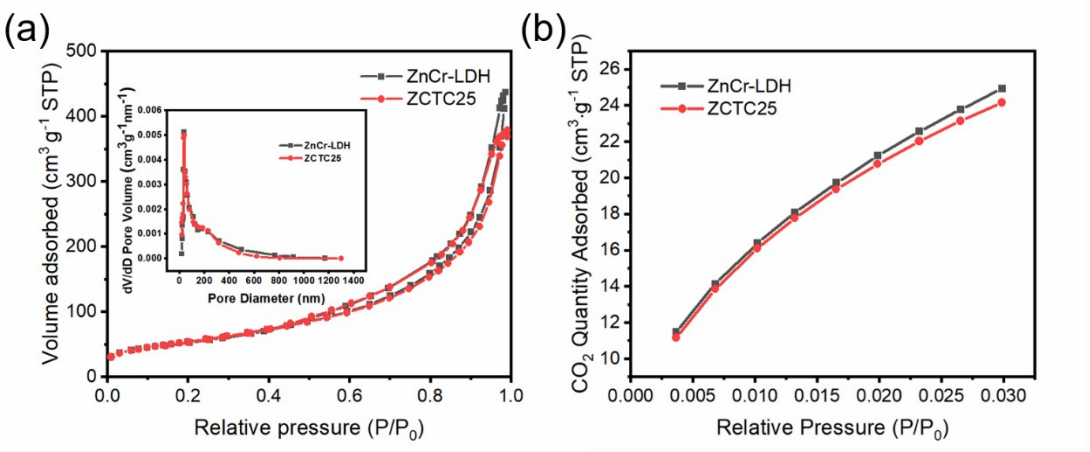

Figure S12. (a) The N_2 adsorption and desorption isotherms and pore size distributions (inset image) of ZnCr-LDH and ZCTC25. (b) The CO_2 adsorption curves of ZnCr-LDH and ZCTC25.

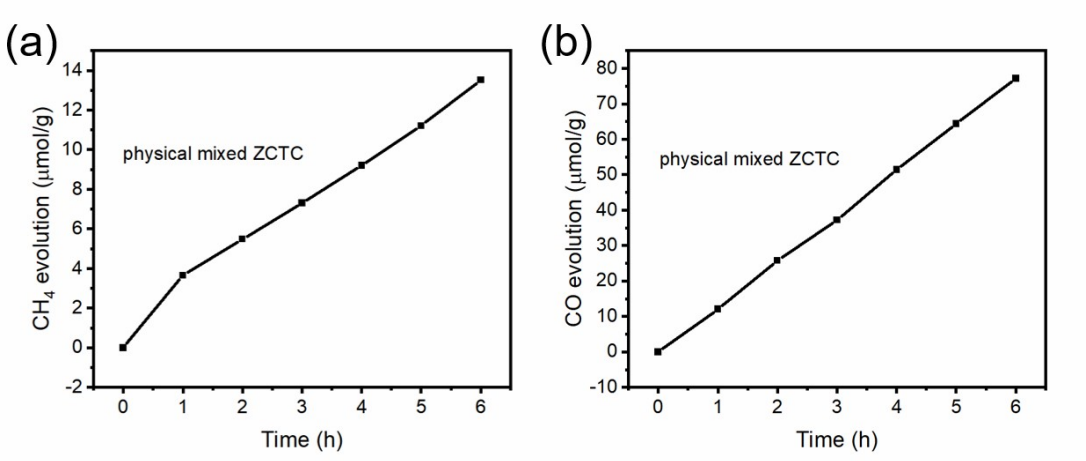

Figure S13. The CO_2 photoreduction performance of composite ZCTC without forming the Schottky junction by physically mixed ZnCr-LDH and $Ti_3C_2T_x$ MXene. (a) CH_4 yields. (b) CO yields.

Table S1. Content of $Ti_3C_2T_x$ MXene in ZCTC composites measured by inductively coupled plasma-optical emission spectrometry.

	ZCTC5	ZCTC25	ZCTC50
$Ti_3C_2T_x$ (wt.%)	0.10	0.51	0.99

Table S2. The results compared with the reported photocatalytic performance of similar composites.

Catalyst	Light source	cocatalyst	Sacrificial agent	Major product evolution rate $\mu mol \cdot g^{-1} \cdot h^{-1}$	Ref.
Ti_3C_2/Bi_2WO_6	Xe lamp			CH_4 1.78 CH_3OH 0.44	[1]
$CdLa_2S_4/Ti_3C_2$	A 300W Xenon lamp equipped with a high-pass filter (λ > 420 nm)		0.25M Na_2SO_3 and 0.35M Na_2S	H_2 11182.4	[2]
0.1Cu_2O@Zn 1.8Cr LDH	200-W Hg-Xe lamp			CO 6.3 μmol (24 h) H_2 3.8 μmol (24 h)	[3]
g-C_3N_4/NiAl-LDH	A 300 W xenon arc lamp with a UV cutoff filter (λ ≥ 420 nm)			CO 8.2	[4]
NiAl-LDH/TNS-75	300 W xenon lamp	$[Ru(bpy)_3]Cl_2 \cdot 6H_2O$	MeCN/TEOA	CO 2128.46	[5]
$ZnIn_2S_4$/ Ti_3C_2	300 W Xe lamp with 420 nm long-pass cutoff filte		TEOA	H_2 3475	[6]
Bi_2MoO_6@MXene	300 W Xe lamp			O_2 734.0	[7]
ZnCr-LDH/$Ti_3C_2T_x$	300 W Xe lamp			CO 122.45 $\mu mol \cdot g^{-1}$ (6 h) CH_4 19.95 $\mu mol \cdot g^{-1}$ (6 h)	This work

References

[1] S Cao, B Shen, T Tong, J Fu, J Yu, Adv. Funct. Mater., 2018, 28, 1800136.

[2] L Cheng, Q Chen, J Li, H Liu, Appl. Catal. B, 2020, 267, 118379.

[3] H Jiang, K Katsumata, J Hong, A Yamaguchi, K Nakata, C Terashima, N Matsushita, M Miyauchi, A Fujishima, Appl. Catal. B, 2018, 224, 783.

[4] S Tonda, S Kumar, M Bhardwaj, P Yadav, S Ogale, ACS Appl. Mater. Interfaces. 2018, 10, 2667.

[5] S Zhao, D Pan, Q Liang, M Zhou, C Yao, S Xu, Z Li, J. Phys. Chem. C, 2021, 125, 10207.

[6] G Zuo, Y Wang, W Teo, A Xie, Y Guo, Y Dai, W Zhou, D Jana, Q Xian, W Dong, Y Zhao, Angew. Chem. Int. Ed., 2020, 59, 11287.

[7] G Zuo, Y Wang, W Teo, A Xie, Y Guo, Y Dai, W Zhou, D Jana, Q Xian, W Dong, Y Zhao, Chem. Eng. J., 2021, 403, 126328.